Indian Journal of Advances in Chemical Science

Article

Fabrication Of Montmorillonite Intercalated Sodium Alginate/Poly (Vinylpyrrolidone-Co-Vinyl Acetate) Beads for Extended Release of Glycopyrrolate

O. Sreekanth Reddy[1], M.C.S. Subha[1]*, C. Madhavi[2], K. Chowdoji Rao[2], B. Mallikarjuna[3]

[1]Department of Chemistry, Sri Krishnadevaraya University, Ananthapuramu, Andhra Pradesh, India, [2]Department of Polymer Science and Technology, Sri Krishnadevaraya University, Ananthapuramu, Andhra Pradesh, India, [3]Department of Chemistry, Government College (A), AKN University, Rajahmundry, Andhra Pradesh, India

ABSTRACT

The aim of the present study was to fabricate nanocomposite clay beads based on sodium alginate/poly (vinylpyrrolidone-co-vinyl acetate)/montmorillonite (MMT) for controlled release of glycopyrrolate (GLY) drug by simple ionotropic gelation technique. The nanocomposite clay beads were obtained. In the present work, we examine the beneficial effects of MMT mineral as drug carrier for GLY because clay minerals play a key role in drug delivery applications. The developed microbeads were characterized by Fourier transform infrared spectroscopy, differential scanning calorimetry, thermogravimetric analysis, X-ray diffraction, energy-dispersive X-ray spectra, and scanning electron microscopy. The effect of MMT content on drug intercalation kinetics, drug encapsulation efficiency and the drug release of the nanocomposite beads were investigated. Drug release kinetics of intercalated GLY has been investigated in both simulated intestinal fluid (pH 7.4) and simulated gastric fluid (pH 1.2) at 37°C and also various kinetic models (zero, first, Higuchi, and Korsmeyer–Peppas) have been used to find out the drug release profile. The drug release studies suggested that controlled release of GLY from nanocomposite beads has been observed during *in vitro* release experiments.

Key words: Sodium alginate, Poly (vinylpyrrolidone-co-vinyl acetate), Montmorillonite, Nanocomposite clay beads, Glycopyrrolate.

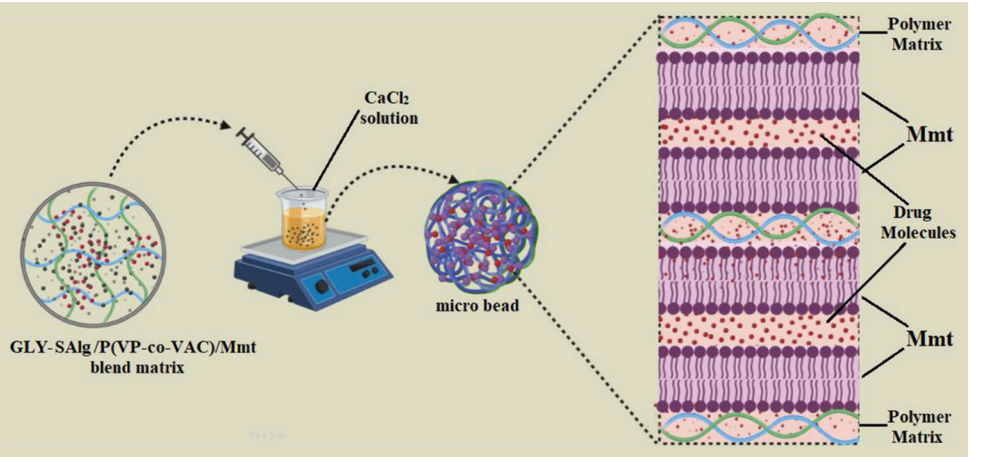

Graphical Abstract

1. INTRODUCTION

Interpenetrating polymer network (IPN) is a clever drug delivery system, with several advantages such as swelling capacity and tremendous mechanical strength, which plays a major role in the targeted and controlled drug delivery [1-3]. The past decades have seen the development of controlled release systems in the fields of medicine and pharmacy because controlled release provides many advantages such as reducing side effects, maintenance of drug concentration at

***Corresponding author:**
E-mail: mcssubha3@gmail.com

ISSN NO: 2320-0898 (p); 2320-0928 (e)
DOI: 10.22607/IJACS.2020.801002

Received: 04th November 2019;
Revised: 06th December 2019;
Accepted: 23rd December 2019

effective levels in plasma, improving the consumption of drug, and decreasing the dosing [4-6].

In IPN drug delivery systems, chemical crosslinkers such as glutaraldehyde and formaldehyde are used to crosslink the polymer matrix for sustained drug release studies. However, the use of chemical crosslinkers leads to adverse side effects such as asthmatic symptoms, rhinitis, and skin irritation [7-9]. To solve this problem, layered silicates such as montmorillonite (MMT), kaolin, palygorskite, and sepiolite are used as a substitute of chemical crosslinkers to decrease the side effects and also increase the efficiency of drug molecules in drug delivery studies [10-12].

MMT is a typical inorganic double layered silicate, which is nanoscale layer in its structure and contains Na^{+}, Ca^{2+}, and Mg^{2+} [13]. It has been used in various fields' catalysis [14], sensors [15], tissue engineering scaffolds [16,17], wound dressing [18,19], nanocomposite drug delivery systems [20,21], and so on. Compared with the palygorskite, MMT makes more suitable candidate for drug loading and drug delivery, since small drug molecules can be successfully intercalated into the interlayer of MMT [22,23]. Previously, a researcher [24] has reported that MMT-PLGA nanocomposites are good oral extended drug delivery vehicle for venlafaxine hydrochloride. Similarly, another researcher [25] also reported that MMT composites are low-cost and attractive drug delivery system intended for intestinal-colonic controlled release.

Glycopyrrolate (GLY) (Figure 1) is a synthetic quaternary ammonium anticholinergic agent similar to atropine and scopolamine [26]. The majority of published articles have exposed the use of this agent at the time of reversal of residual neuromuscular block and have shown that, because of the synchronous actions of GLY and the anticholinesterase neostigmine, changes in heart rate during reversal with GLY-neostigrnine combinations are much less than those associated with atropine-containing mixtures [27]. GLY can be used to treat various gastrointestinal disorders, and during the past decade it has been used as a preanesthetic agent, most of the studies have revealed that it can be produced powerful antisialagogue effects without extreme changes in heart rate [1,28].

Sodium alginate (SAlg) is an anionic linear hetero polysaccharide contains alternating blocks of β (1–4) D-mannuronic acid and α (1–4) L-glucuronic acid residue (Gomez *et al*., 2017). SAlg when interact ionically with multivalent cations (e.g., Ca^{2+}, Mg^{2+}, and Ba^{2+}), then the L-glucuronic acid groups can connect with each other, resulting in a three-dimensional hydrogel network which has pH-sensitive property. SAlg acts as a carrier in drug delivery due to its biocompatibility, hydrophilicity, biodegradability, and mechanical strength [29]. MMT-blended alginate offers many advantages such as reduce the drug release rate by increasing the drug adsorption capacity in the matrix and increase the drug encapsulation [30]. SAlg was not intercalated into MMT, due to the repulsive forces between negatively charged clay surfaces and carboxylic groups of polymer [31]. However, the negative charge of alginate carboxyl groups interacts electrostatically with the positively charged sites existing at the edges of MMT, which brought about numerous contact points and created a three-dimensional network. If MMT content increases, the SAlg chain acts as a bridge between neighboring silicate layers [32,33].

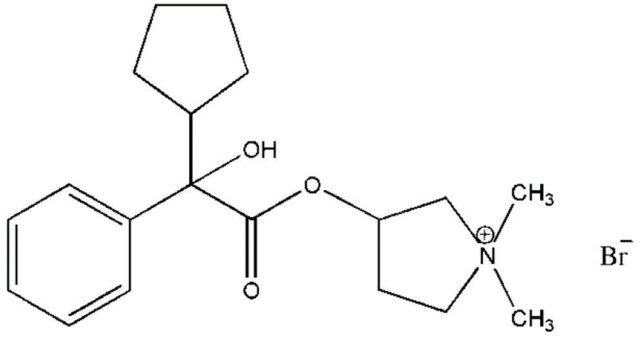

Figure 1: Structure of glycopyrrolate.

Poly vinylpyrrolidone-co-vinyl acetate (P(VP-co-VAC)) block copolymer comprising both hydrophilic part (poly vinylpyrrolidone) and hydrophobic part (poly vinyl acetate). P(VP-co-VAC) is an attractive polymer for many applications such as pervaporation, drug delivery, and tissue engineering [34]. It could effectively solubilize the hydrophobic drugs due to the presence of hydrophobic part in the polymer chain, therefore it should be an interesting candidate as a drug carrier for hydrophobic drugs [35].

A few articles have been reported the combination of MMT and SAlg for controlled drug delivery [24,30,31,33], but the best of our knowledge, the use of SAlg/P(VP-co-VAC)/MMT microbeads for controlled release of GLY has not yet been investigated. In view of above information, the objective of the present work is to prepare SAlg/P(VP-co-VAC)/MMT microbeads for controlled release of GLY.

2. EXPERIMENTAL

2.1. Materials

SAlg, P(VP-co-VAC), and MMT are purchased from Sigma-Aldrich (USA). Calcium chloride was purchased from S.D. Fine chemicals, Mumbai, India. Glycopyrrolate received as a gift sample from M/s Suven Life Sciences Ltd. Hyderabad, India. Water used was of high purity grade after double distillation.

2.2. Preparation of SAlg/MMT/P(VP-co-VAC) Microbeads

GLY (150 mg) was added gradually to a blend suspension of SAlg/P(VP-co-VAC) with or without MMT (amounts as given in Table 1) in double distilled water (20 mL) and stirred for 10 h at room temperature. Afterward, the suspension was placed in sonication for 30 min at 40°C to get homogenous suspension. There after the resulting suspension was slowly dropped into $CaCl_2$ solution, where the spherical beads formed instantly were kept for 30 min. The obtained wet beads were collected by decantation, washed 3 times with double distilled water to remove the drug attached on the bead surface, and finally were dried in air overnight at room temperature.

3. CHARACTERIZATIONS METHODS

3.1. Ultraviolet (UV)-visible Spectrum Analysis of GLY

10 mg of GLY dissolved in 10 mL of 0.1 NaOH, and this was transferred into a 100 mL standard flask. The volume was brought up to the mark with 0.1 NaOH to obtain a stock solution of GLY with 100 µg/ml final concentration. 2 ml sample was transferred into a 10 mL standard flask and the volume was made up to the mark with 0.1 NaOH to prepare a concentration of 20 µg/mL. The sample was further scanned by a UV-visible spectrophotometer (Lab India, Mumbai, India) in the range of 200–400 nm, using 0.1 NaOH as a blank.

3.2. Intercalation Kinetics

To determine the optimal time required for maximum intercalation of GLY with MMT. A known amount of GLY (30 mg) and MMT (100 mg) were mixed into 30 mL of double distilled water with continuous stirring at 37°C. At regular intervals of time (0.5, 1, 2, 4, 8, and 14 h), the reaction mixture was filtered and concentration of GLY was analyzed using UV-Vis spectrophotometer at fixed λ_{max} value of 224.60 nm.

Table 1: Formulation, composition, and % encapsulation efficiency of all samples.

Formulation	SAlg (W/v %)	P(VP-co-VAC) (W/v %)	MMT (Wt %)	Drug (mg)	%EE±S.D
SA	100	00	00	150	60.7±1.4
SP	80	20	00	150	62.4±2.3
SPM4	80	20	0.4	150	67.8±0.7
SPM6	80	20	0.6	150	69.3±1.9
SPM8	80	20	0.8	150	71.4±0.8
Placebo	80	20	00	00	00
Placebo-MMT	80	20	0.4	00	00

SAlg: Sodium alginate, P(VP-co-VAC): Poly vinylpyrrolidone-co-vinyl acetate, MMT: Montmorillonite, EE: Encapsulation efficiency

3.3. Effect of pH

The experiments were performed to estimate the most favorable pH for the intercalation of GLY with MMT. For this purpose, a known amount of GLY (30 mg) and MMT (100 mg) were dissolved into 30 mL of different pH solutions (2.0, 4.6, 6.0, 7.4, 8.5, and 10.5) and stirred at 300 rpm for 1 h at 37°C. The solution was then filtered and concentration of GLY in the filtrate was analyzed by UV spectrophotometer (Lab India, Mumbai, India) at the λ_{max} of 224.60 nm.

3.4. Fourier Transform Infrared (FTIR) Analysis

FTIR spectra of SAlg, P(VP-co-VAC), MMT, GLY, placebo, SA, SP, placebo-MMT, and SPM6 were measured as pellets in KBr with a FTIR spectrophotometer (model Bomem MB-3000, with Horizon MB™ FTIR software) in the wavelength range of 400–4000 cm^{-1} to find out the possible chemical interactions between polymers, MMT, and drug.

3.5. X-ray Diffraction (X-RD) Analysis

The X-RD of GLY, placebo, SP, placebo-MMT, SPM6, and pure MMT was performed by a wide angle X-ray scattering diffractometer (Panalytical X-ray Diffractometer, model: Rigaku Ultima IV Powder XRD) with CuKα radiation (λ=1.54060) at a scanning rate of 10/min to determine the crystallinity.

3.6. Scanning Electron Microscopy (SEM) Analysis

The morphological characterization of microbeads was observed using SEM (JEOL JSM-7100F) with an accelerated voltage of 20 kV equipped with an energy-dispersive X-ray spectra (EDS) detector.

3.7. Determination of Encapsulation Efficiency (EE)

%EE of all formulations was estimated by the following procedure. Weigh accurately 10 mg of microbeads and immersed into 100 mL of pH 7.4 phosphate buffer solution containing 5% ethyl alcohol for 24 h. Afterward, the solution was placed for sonication for 10 min to ensure the complete extraction of drug from the microbeads. The filtrate was assayed using UV-visible spectrophotometer at the λ_{max} of 224.60 nm with pH 7.4 buffer solution as a blank. The percentage of drug loading and % EE was calculated using the following equations.

$$\text{Drug loading } (\%) = \frac{\text{Weight of drug in microbeads}}{\text{weight of microbeads}} \times 100$$

$$\text{EE } (\%) = \frac{\text{Actual drug loading}}{\text{Theortical drug loading}} \times 100$$

3.8. Swelling Studies

The swelling behavior of different formulations was determined gravimetrically in simulated intestinal fluid (pH 7.4) and simulated gastric fluid (pH 1.2) at 37°C. The % of equilibrium swelling degree was calculated using the following equation:

$$\%\ \text{swelling degree} = \frac{W_s - W_d}{W_d} \times 100$$

Where W_s is the weight of swollen beads and W_d is the weight of dry beads.

3.9. In vitro Drug Release Studies

To study the *in vitro* drug release studies of different formulations were performed at 37°C using a dissolution tester (Lab India, Mumbai, India). Weight accurately 100 mg of microbeads and dispersed into 900 mL of pH 7.4 and pH 1.2 phosphate buffer solutions and stirred at a rotation speed of 50 rpm. At regular intervals of time, aliquot samples were withdrawn, and analyzed using UV-visible spectrophotometer at fixed λ_{max} value of 224.60 nm. Same amount of withdrawn sample was added to maintain sink condition.

3.10. Drug Release Kinetics

The drug release kinetics was analyzed by fitting the data in to kinetic models, which include zero-order, first-order, Higuchi, and Korsmeyer–Peppas [36]. Based on the goodness of data fit, the highest correlation coefficient was indicative of best-fit model to describe drug release kinetics [37].

4. RESULTS AND DISCUSSION

4.1. UV-visible Spectrum Analysis of GLY

The GLY solution was scanned by a UV-visible spectrophotometer in the range of 200–400 nm, using 0.1 NaOH as a blank. The maximum absorbance (λ_{max}) of GLY solution was found to be 224.60 nm. This was further utilized to obtain a calibration curve.

4.2. Intercalation Kinetics

Intercalation kinetics reveals that the time required for intercalation of GLY with MMT by a rapid ion-exchange process between sodium ions of MMT and cations of GLY molecules. From Figure 2, it was clear that 13.7 % of GLY was intercalated in interlayer of MMT within 1 h, and remains constant up to 14 h. Therefore, we should keep 1 h time for interaction between GLY and MMT to avoid partial interaction in the following experiments.

4.3. Effect of pH

The effect of pH on the intercalation of GLY into the interlayer of MMT is displayed in Figure 3. The results reveal that suitable pH range

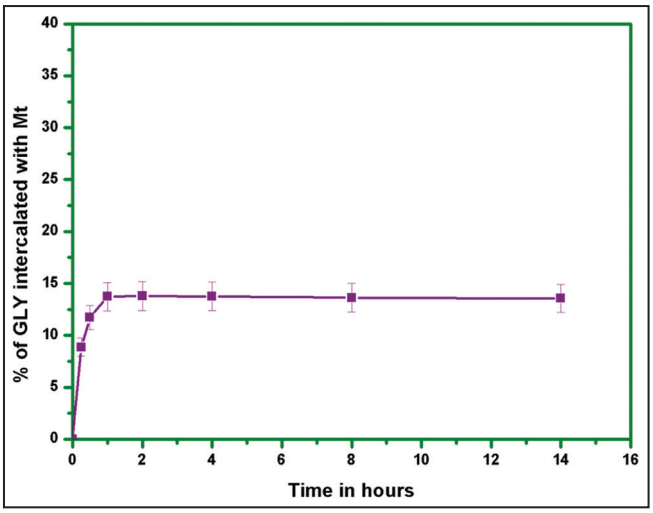

Figure 2: Effect of time for intercalation of glycopyrrolate with montmorillonite.

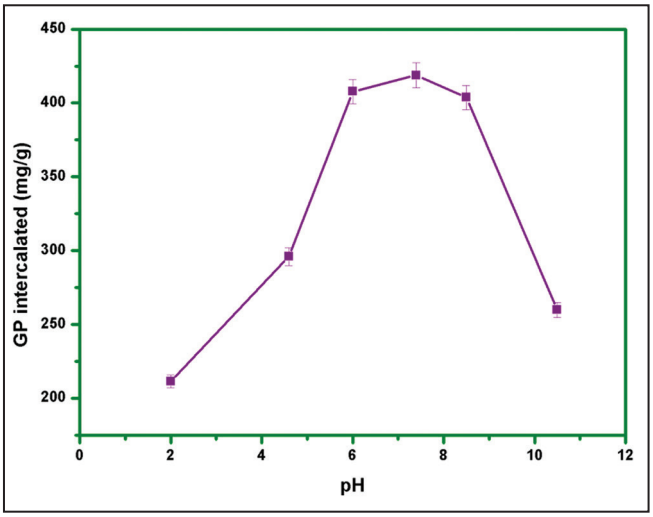

Figure 3: Effect of pH on intercalation of glycopyrrolate into montmorillonite.

for intercalation of GLY with MMT is 6.0–8.5, because at this range intercalation of GLY almost linear. At pH below 6.0, there was a sharp decrease in intercalation of GLY in MMT layer. Basically, GLY contains permanent positive charge; therefore, at pH below six competitions arise between cationic drug and H^+ ions of MMT layer, which leads to steep decrease in intercalation of GLY with MMT clay lattice [38]. At pH above 8.5, there was a steep decrease in intercalation of GLY with MMT, this is due to the presence of largely uncharged GLY species, confirms that cation exchange was no long domination [39]. From this, we can conclude intercalation of GLY in MMT is higher in the pH range 6.0–8.5, this is due to attraction between positive charge of GLY and negative charge of MMT.

4.4. FTIR Analysis

The FTIR spectra of SAlg, GLY, SA, P(VP-co-VAC), placebo, and SP are displayed in Figure 4. The FTIR spectra of SAlg show a characteristic peaks at 3409 cm^{-1} (O–H stretching frequency), 1596 cm^{-1} (asymmetric C–O–C stretching frequency), 1388 cm^{-1} (symmetric C–O–C stretching frequency), and 1110 cm^{-1} (C–O stretching frequency) [40]. The FTIR spectra of GLY show a distinct peaks at 3332 cm^{-1} (O–H stretching frequency), 2962 cm^{-1} (alkane C–H stretching frequency), 1735 cm^{-1} (C=O stretching frequency), 1596

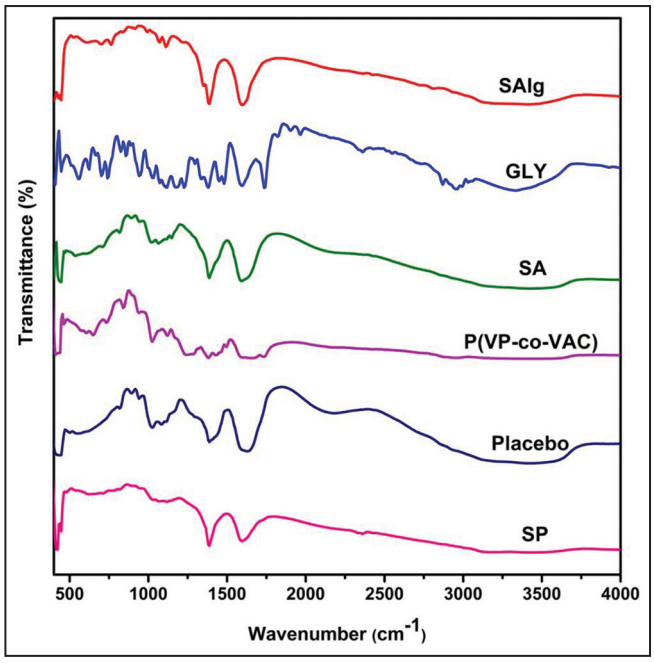

Figure 4: Fourier transform infrared spectrum of sodium alginate, glycopyrrolate, SA, poly vinylpyrrolidone-co-vinyl acetate, placebo, and SP.

and 1481 cm^{-1} (aromatic C=C stretching frequency), 1380 cm^{-1} (C–H bending frequency), and 1118 cm^{-1} (C–N stretching frequency) [41]. On comparing, the FTIR spectra of SAlg and SA the carbonyl stretching frequency of pure SAlg are decreased from 1596 cm^{-1} to 1589 cm^{-1}, suggesting that drug should be interacted with the polymer matrix. The FTIR spectra of P(VP-co-VAC) show a characteristic peaks at 3394 cm^{-1} (O–H stretching frequency), 1735 and 1635 cm^{-1} (C=O stretching frequency), 1380 cm^{-1} (C–H bending frequency), 1242 cm^{-1} (C–N stretching frequency), and 1026 cm^{-1} (C–O stretching frequency of ester group) [42]. On comparing the FTIR spectra of placebo and SP, the C=O stretching frequency of placebo microbeads is decreased from 1609 cm^{-1} to 1596 cm^{-1} due to intermolecular bonding between drug and polymer matrix, which indicates drug should be loaded in the microbeads.

The FTIR spectra of placebo, pristine MMT, placebo-MMT, and SPM6 are displayed in Figure 5. The FTIR spectrum of MMT shows distinct peaks at 3685 and 3583 cm^{-1} (O–H stretching frequency of Si-OH and Al–Al–OH), 3379 cm^{-1} (H–O–H stretching frequency of interlayer water), 1627 cm^{-1} (H–O–H bending mode of adsorbed water), 1380, 1002 and 931 cm^{-1} corresponds to (Si–O–Si) stretching band, and 794 and 509 cm^{-1} attributes to O–Si–O and Al–Si–O bending vibrations [43-45]. On comparing the FTIR spectra of placebo-MMT with MMT, the O–H stretching frequency of Si–OH at 3616 cm^{-1} is disappeared in the spectra of MMT placebo microbeads, which confirms the interaction takes place between polymer matrix and MMT. And also, the O–H stretching frequency at 3440 cm^{-1} was shifted to lower frequency, which indicates the intermolecular hydrogen bonding between polymer matrix and MMT clay [33]. On comparing the FTIR spectra of placebo with placebo-MMT, the asymmetric stretching of –COOH is decreased from 1609 cm^{-1} to 1606 cm^{-1}, suggesting that MMT is interacted with polymer matrix, and also a band appears at 520 cm^{-1} indicating the presence of MMT composition in the matrix. On comparing the FTIR spectra of placebo-MMT with SPM6, the stretching frequency at 1606 cm^{-1} in placebo-MMT is lowered in the case of SPM6 because the drug should be intercalated with hydroxyl

groups of MMT in microbeads, which confirms that the drug is loaded in microbeads.

4.5. X-RD Analysis

To examine the physical state of the drug in the microbeads, XRD analysis was performed. Figure 6 presents the XRD patterns of GLY, placebo, SP, placebo-MMT, SPM6, and pure MMT. The XRD pattern of GLY shows a characteristic peaks at 2θ of 10.6° and 21.4° represent the crystalline nature of GLY. On the other hand, no such characteristic peak was observed in the case of the SP, this suggests that the drug has molecularly dispersed in the microbeads. The XRD patterns of MMT show a characteristic peaks at 19.8°, 26.6°, and 34.9° represent the crystalline nature of MMT. Whereas these peaks were appeared in placebo-MMT and SPM6, but the intensity of these peaks was decreased, which confirms the MMT intercalated with active sites of polymer and drug molecules. On comparing placebo-MMT with SPM6, a peak at 26.8° in placebo-MMT will be shifted to 26.7° in SPM6, which indicates the MMT intercalated with the drug molecules. The basal space of placebo-MMT at 2Θ value of 26.8° is 3.326 nm whereas the basal space of SPM6 at 2Θ value of 26.7° is 3.339 nm; consequently, the basal space is decreased in SPM6, which confirms that the GLY is intercalated with MMT. The basal space values are calculated using the following equation.

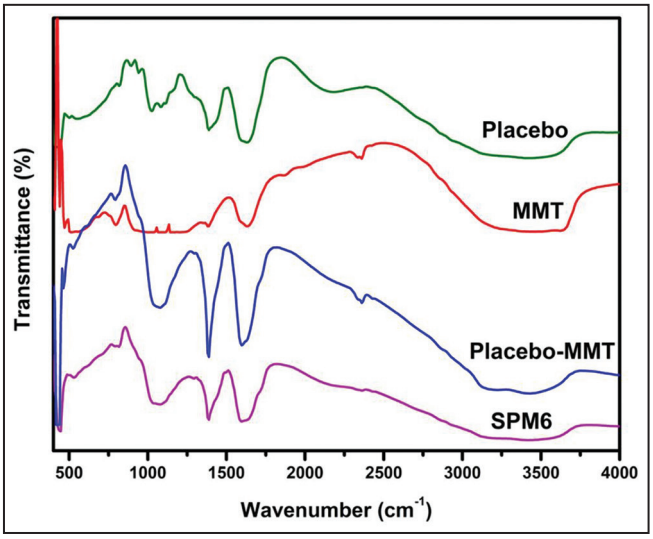

Figure 5: Fourier transform infrared spectrum of placebo, montmorillonite (MMT), placebo-MMT and SPM6.

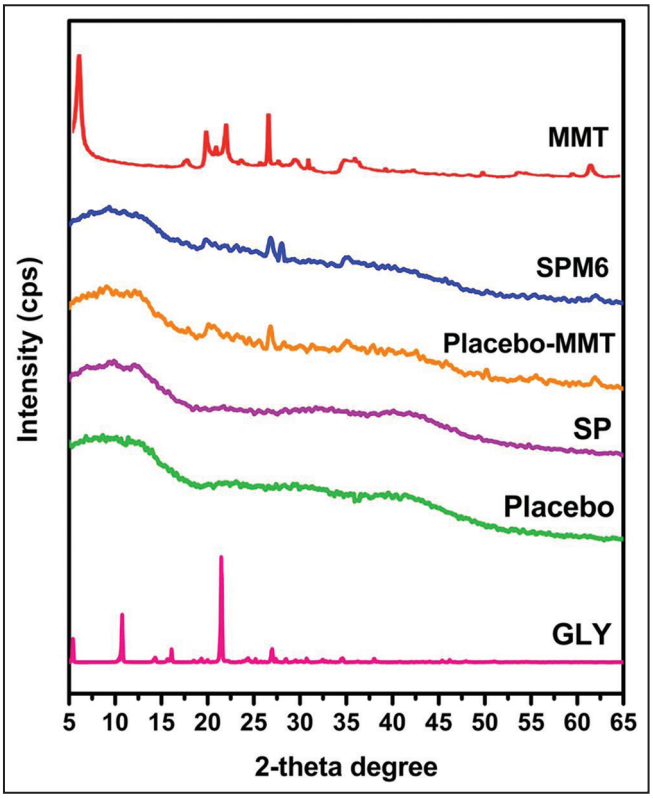

Figure 6: Powder X-ray diffraction patterns of pristine glycopyrrolate, placebo, SP, placebo-montmorillonite (MMT), SPM6, and MMT.

Bragg's equation: $2d \sin\Theta = n\lambda$

4.6. SEM Analysis

To examine the surface morphology and chemical composition of microbeads, field emission scanning electron microscope and EDS analysis were performed. From Figure 7a, it was clearly observed that the microbeads have rough surface with visible wrinkles. In SPM6, it was observed that high roughness is present, which indicates the presence of MMT platelets on outer surface of microbeads. And also, SPM6 microbeads are more spherical in shape than the placebo microbeads. This is due to the presence of MMT, because it acts as a physical crosslinker in the matrix, which enhances the dimensional stability and form a three-dimensional spherical shape network. These results suggesting that the MMT was successfully loaded in the developed microbeads. From the results of SEM images, the average sizes of microbeads were found to be 1100–1300μm.

The EDS (Figure 7b) analysis shows the presence of C, N, and O elements in the placebo microbeads and SP. Nitrogen peak was observed in all microbeads this is due to the presence of P(VP-co-VAC) polymer in the matrix, but the intensity of nitrogen peak was high in the case of drug loaded microbeads, which confirms that the drug is loaded in the microbeads. Whereas in drug loaded MMT microbeads the additional signals corresponding to the Si and Al elements were detected, which confirms the MMT intercalates with the polymer matrix.

4.7. Differential Scanning Calorimetry (DSC) and Thermogravimetric Analysis (TGA)

Figure 8a shows the DSC thermograms of GLY, placebo, and SP microbeads. DSC curve of GLY shows a sharp peak at 200.4°C and a broad peak at 278.1°C because of its melting temperature. On the other hand, no such peak was observed in the case of the SP, which confirmed that GLY was molecularly dispersed in the microbeads. The TGA thermograms of GLY, placebo, and SP are displayed in Figure 8b. The TGA thermogram of GLY should remain stable up to 198°C, after that it follows mass loss and being maximum at 335°C due to total degradation of the compound. The thermal decomposition of placebo occurs in three consecutive steps. The first weight loss of 34 % was found in between 35 and 179°C, is due to loss of adsorbed water. The second weight loss 20% was observed in the region of 193–279°C, followed by weight loss of 14% in between the region of 301 and 600°C is due to degradation of polymer matrix. In the case of SP three weight loss steps was observed. The first weight loss 27 % was observed in the region of 37–180°C, followed by weight loss of 23% in between the region of 191 and 301°C is due to degradation of polymer matrix. The last with weight loss of 12% in the region of 309–600°C, corresponds to complete decomposition of polymer network. The TGA results suggest that developed microbeads shows an overall improvement in the thermal stability.

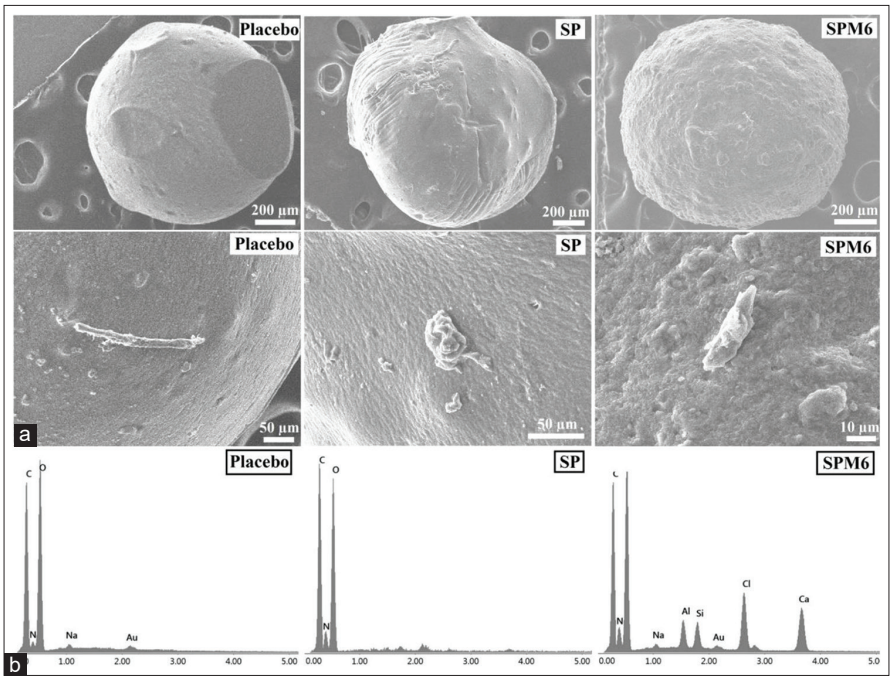

Figure 7: (a) Field emission scanning electron microscope and (b) energy-dispersive X-ray spectra analysis of placebo, SP, and SAMP6 formulations.

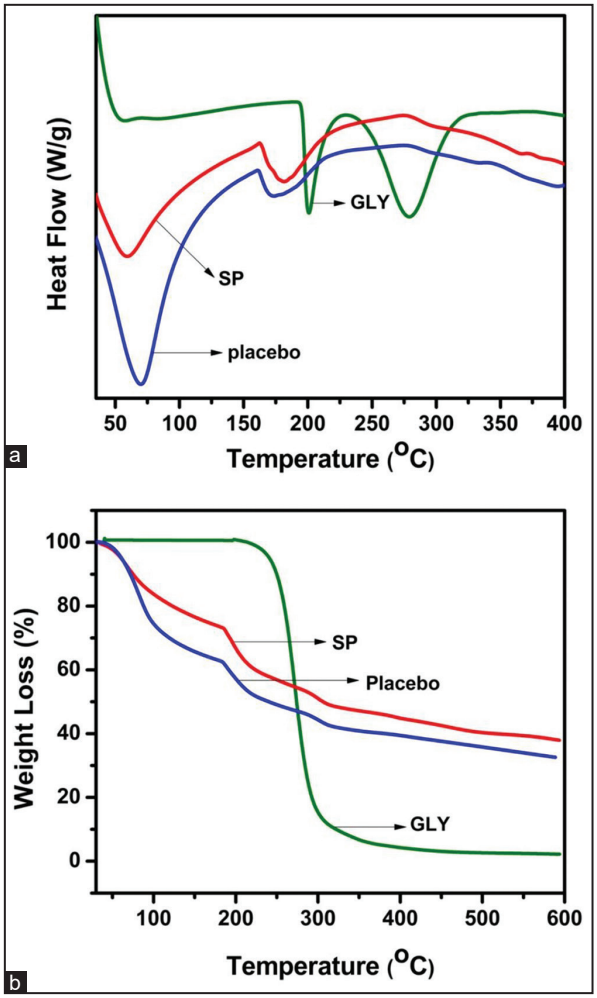

Figure 8: Thermal analysis of glycopyrrolate, placebo, and SP microbeads (a) differential scanning calorimetry and (b) thermogravimetric analysis

4.8. Swelling Degree

Swelling degree is one of the important factors to understand release characteristics through microbeads. To find out the effect of pH on swelling degree, we have performed swelling studies at pH 7.4 (simulated intestinal fluid) and pH 1.2 (simulated gastric fluid) at 37°C and the results are presented in Figure 9. From Figure 10, it was clearly observed that the swelling degree is more at pH 7.4 than at pH 1.2 because at low pH hydrogen bonding interactions were developed between –COOH groups of polymer matrix and solvent molecules, which results shrinkage of polymer network subsequently swelling ratio was decreased. Hence, the developed microbeads are potentially good carriers to deliver drug molecules at intestine and to avoid gastric release of drugs.

4.9. Determination of %EE

From the drug encapsulation studies, it was observed that the % EE was found to be around 60–71 % (Table 1), which is dependent on percentage of MMT present in the polymer matrix. By increasing the amount of MMT in the polymer matrix, the GLY EE also increases this is due to MMT has large specific area and good absorption capacity, so it can absorb GLY well. Moreover, % EE increases with increasing the amount of MMT, this is due to a strong hydrogen bonding between GLY and hydroxyl groups present on surface of MMT [33].

4.10. In vitro Drug Release Studies

In vitro release studies were carried out in phosphate buffer media (pH 7.4 and 1.2) to understand the GLY release from drug loaded microbeads. From Figure 10, it was observed that the release rate is high at pH 7.4 than the pH 1.2. These results are correlated with swelling behavior in response to the pH. At pH 1.2, the release of GLY is low due to less expansion of network; hence, the entrapped drug molecules are difficult to transport in to the buffer media. Whereas at pH 7.4, the carboxylic groups show less interactions with buffer media consequently the network becomes more loose, hence the entrapped drug molecules easily leaches out from the network.

The formulation SA shows high release rate (92%) compared to SP (81%) within the same time, because the presence of hydrophobic part

Table 2: Release rate constant and correlation coefficient of all formulations after fitting of drug release data into different mathematical models.

Sample	Zero-order		First-order		Higuchi		Korsmeyer–Peppas	
	k0	r2	k1	r2	KH	r2	n	r2
SA	28.445	0.829	1.887	0.950	7.046	0.949	0.486	0.964
SP	24.632	0.844	1.886	0.941	9.698	0.950	0.428	0.939
SPM4	16.009	0.953	1.932	0.986	3.410	0.997	0.436	0.997
SPM6	12.371	0.873	1.950	0.993	0.899	0.994	0.461	0.991
SPM8	10.895	0.980	1.956	0.993	0.484	0.993	0.466	0.995

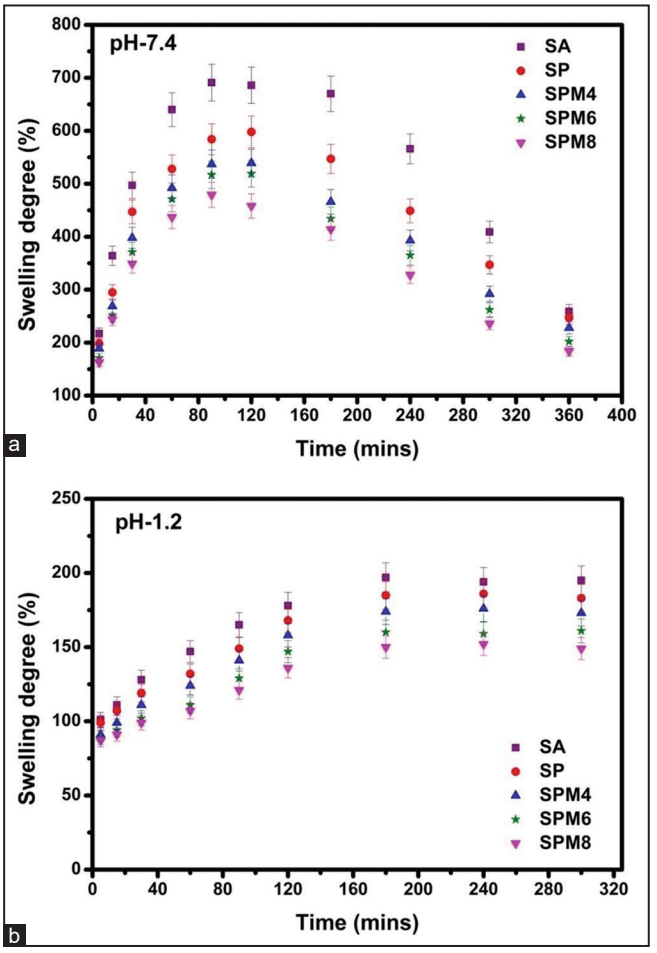

Figure 9: Swelling studies of all formulations at (a) pH-7.4 and (b) pH-1.2 at 37°C.

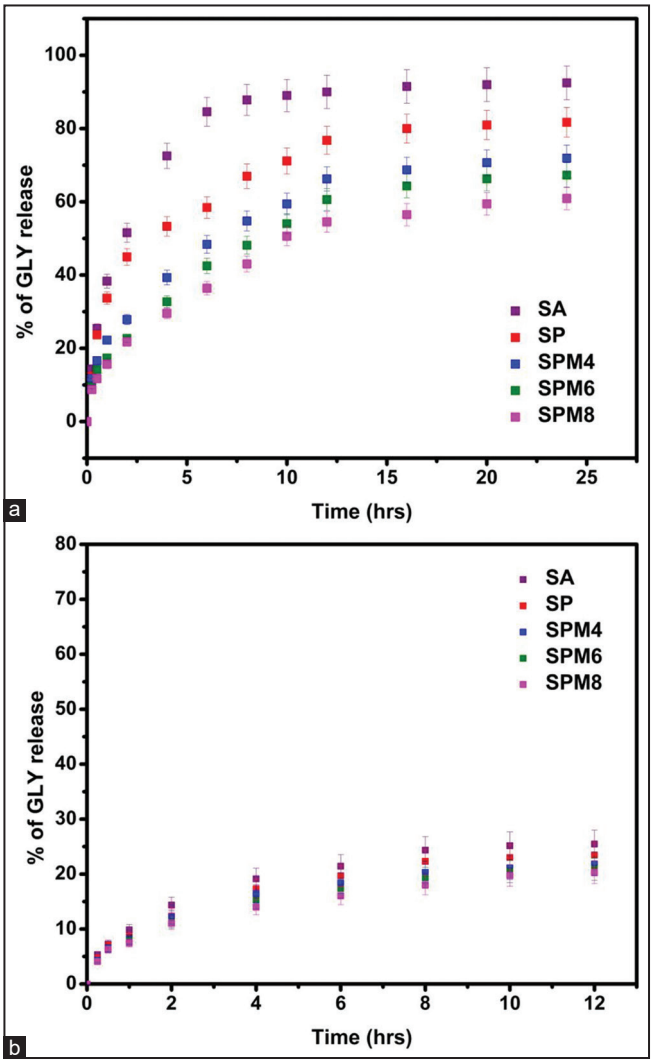

Figure 10: *In vitro* release of glycopyrrolate through SA/poly vinylpyrrolidone-co-vinyl acetate/montmorillonite microbeads at (a) pH 7.4 and (b) pH 1.2 at 37°C.

in P(VP-co-VAC) decreases the diffusion of the drug molecules into the media. As a result, it controls the drug release rate and burst release of the drug in comparison with SP. The release rate of GLY from the microbeads containing MMT is decreased as the concentration of MMT increases; this is due to interlayer cations cannot be exchanged completely in ion exchange process between the intercalated drug molecules and the phosphate ions of the buffer solution [23,46,47]. And also, an electrostatic attraction develops between protonated amino groups of GLY and anionic groups of MMT layer, which leads to incomplete drug release process [48,49].

4.11. Drug Release Kinetics

To find out the drug release mechanism, the data obtained from *in vitro* drug release studies in phosphate-buffered saline (7.4) were fitted into different kinetic models including zero-order, first-order, Higuchi, and Korsmeyer–Peppas models which are empirical in nature, the results of rate constant and correlation coefficient (r^2) of all formulations are displayed in Table 2. The r^2 values were close to first-order and Higuchi models. Hence, the drug release kinetics follows either first-order or Higuchi model. According to Higuchi model, the drug release from the microparticles involves the penetration of liquid into the matrix and dissolves the drug, which then diffuses the drug into the exterior liquid through pores or intestinal channels. According to first-order kinetics,

the drug release process is directly proportional to drug content involved in the process. Therefore, rate of process increases linearly with concentration of drug increases. Further, the type of diffusion was revealed by Korsmeyer–Peppas model. The first 60% drug release data were fitted into Korsmeyer–Peppas model.

$$\frac{M_t}{M_\infty} = kt^n$$

Where, Mt/Mα represents the fractional drug release at time t, k is a constant characteristic of the drug-polymer system, and n is the release exponent indicating the type of drug release mechanism. The values "n" (Table 2) are obtained in the range of 0.428–0.466 indicates Fickian type of diffusion process [25].

5. CONCLUSION

In the present study, MMT intercalated SA/P(VP-co-VAC) microbeads were developed by simple ionotropic gelation method for the extended release of GLY. Microbeads formation was confirmed by FTIR spectroscopy. DSC and TGA studies confirmed the chemical stability and molecular level dispersion of GLY in microbeads, respectively. XRD studies reveal that the MMT intercalates with active sites of polymer molecules and drug molecules and also it reveals the molecular level dispersion of GLY. SEM study reveals that the MMT platelets are present on the surface of microbeads. The *in vitro* release study reveals that MMT containing microbeads shows a controlled release of GLY. The *in vitro* results were fitted into Peppas equation and the results showed that the drug mechanism followed non-Fickian type of diffusion mechanism. Based on the results, it was concluded that the developed MMT microbeads are good promising candidate for novel drug delivery systems.

6. ACKNOWLEDGMENTS

One of the authors (M.C.S. Subha) thanks the University Grants Commission for providing financial support under the UGC-BSR faculty fellowship (Reference No: 201920-BSRFACULTY-10094-4), Government of India, New Delhi.

7. CONFLICTS OF INTEREST

The authors have indicated that they have no conflicts of interest regarding the content of this article.

8. REFERENCES

1. T. Ali-Melkkilä, T. Kaila, J. Kanto, (1989) Glycopyrrolate: Pharmacokinetics and some pharmacodynamic findings, ***Acta Anaesthesiologica Scandinavica***, **33**: 513-517.
2. C. Chen, Z. Gao, X. Qiu, S. Hu, (2013) Enhancement of the controlled-release properties of chitosan membranes by crossslinking with suberoyl chloride, ***Molecules***, **18**: 7239-7252.
3. N. S. Reddy, K. S. V. Rao, S. Eswaramma, K. M. Rao, (2016) Development of temperature-responsive semi-IPN hydrogels from PVA-PNVC-PAm for controlled release of anti-cancer agent, ***Soft Materials***, **14**: 96-106.
4. Z. S. Patel, M. Yamamoto, H. Ueda, Y. Tabata, A. G. Mikos, (2008) Biodegradable gelatin microparticles as delivery systems for the controlled release of bone morphogenetic protein-2, ***Acta Biomaterialia***, **4**: 1126-1138.
5. K. M. Reddy, V. R. Babu, K. S. V. Rao, M. C. S. Subha, K. C. Rao, M. Sairam, T. M. Aminabhavi, (2008)Temperature sensitive semi-IPN microspheres from sodium alginate and N-isopropylacrylamide for controlled release of 5-fluorouracil, ***Journal of Applied Polymer Science***, **107**: 2820-2829.
6. K. S. V. Krishna Rao, A. B. V. Kiran Kumar, K. M. Rao, M. C. S. Subha, Y. I. Lee, (2008) Semi-IPN hydrogels based on poly(vinyl alcohol) for controlled release studies of chemotherapeutic agentand their swelling characteristics, ***Polymer Bulletin***, **61**: 81-90.
7. A. Pinheiro, A. Cooley, J. Liao, R. Prabhu, S. Elder, (2016) Comparison of natural crosslinking agents for the stabilization of xenogenic articular cartilage, ***Journal of Orthopaedic Research***, **34**: 1037-1046.
8. T. Takigawa, Y. Endo, (2006) Effects of glutaraldehyde exposure on human health, ***Journal of Occupational Health***, **48**: 75-87.
9. E. Esposito, R. Cortesi, C. Nastruzzi, (1996) Gelatin microspheres: Influence of preparation parameters and thermal treatment on chemico-physical and biopharmaceutical properties, ***Biomaterials***, **17**: 2009-2020.
10. Y. Zhang, M. Long, P. Huang, H. Yang, S. Chang, Y. Hu, A. Tang, L. Mao, (2017) Intercalated 2D nanoclay for emerging drug delivery in cancer therapy, ***Nano Research***, **10**: 2633-2643.
11. J. H. Yang, J. H. Lee, H. J. Ryu, A. A. Elzatahry, Z. A. Alothman, J. H. Choy, (2016) Drug-clay nanohybrids as sustained delivery systems, ***Applied Clay Science***, **130**: 20-32.
12. J. Zheng, J. Shan, Z. Fan, K. Yao, (2011) Preparation and properties of gelatin-chitosan/montmorillonite drug-loaded microspheres, ***Journal of Wuhan University of Technology-Mater. Sci. Ed***, **26**: 628-633.
13. J. Zhang, S. Xu, Z. Du, K. Ren, (2011) Preparation and characterization of montmorillonnite/tamarind gum/ sodium alginate composite gel beads, ***Journal of Composite Materials***, **45**: 295-305.
14. S. Yoda, Y. Sakurai, A. Endo, T. Miyata, H. Yanagishita, K. Otake, T. Tsuchiya, (2004) Synthesis of titania-pillared montmorillonite via intercalation of titanium alkoxide dissolved in supercritical carbon dioxide, ***Journal of Materials Chemistry***, **14**: 2763-2767.
15. A. de Barros, C. J. L. Constantino, N. C. da Cruz, J. R. R. Bortoleto, M. Ferreira, (2017) High performance of electrochemical sensors based on LbL films of gold nanoparticles, polyaniline and sodium montmorillonite clay mineral for simultaneous detection of metal ions, ***Electrochimica Acta***, **235**: 700-708.
16. A. A. Haroun, A. Gamal-Eldeen, D. R. K. Harding, (2009) Preparation, characterization and *in vitro* biological study of biomimetic three-dimensional gelatin-montmorillonite/cellulose scaffold for tissue engineering, ***Journal of Materials Science: Materials in Medicine***, **20**: 2527-2540.
17. J. P. Zheng, C. Z. Wang, X. X. Wang, H. Y. Wang, H. Zhuang, K. D. Yao, (2007) Preparation of biomimetic three-dimensional gelatin/montmorillonite-chitosan scaffold for tissue engineering, ***Reactive and Functional Polymers***, **67**: 780-788.
18. V. Ambrogi, D. Pietrella, M. Nocchetti, S. Casagrande, V. Moretti, S. De Marco, M. Ricci, (2017) Montmorillonite-chitosan-chlorhexidine composite films with antibiofilm activity and improved cytotoxicity for wound dressing, ***Journal of Colloid and Interface Science***, **491**: 265-272.
19. S. Noori, M. Kokabi, Z. M. Hassan, (2015) Nanoclay enhanced the mechanical properties of poly(vinyl alcohol)/chitosan/ montmorillonite nanocomposite hydrogel as wound dressing, ***Procedia Materials Science***, **11**: 152-156.
20. N. Salahuddin, A. Elbarbary, N. G. Allam, A. F. Hashim, (2014) Polyamide-montmorillonite nanocomposites as a drug delivery system: Preparation, release of 1,3,4-oxa(thia)diazoles, and

antimicrobial activity, ***Journal of Applied Polymer Science***, **131**: 41177.
21. X. Wang, Y. Du, J. Luo, (2008) Biopolymer/montmorillonite nanocomposite: Preparation, drug-controlled release property and cytotoxicity, ***Nanotechnology***, **19**: 065707.
22. R. Wang, Y. Peng, M. Zhou, D. Shou, (2016) Smart montmorillonite-polypyrrole scaffolds for electro-responsive drug release, ***Applied Clay Science***, **134**: 50-54.
23. G. V. Joshi, B. D. Kevadiya, H. A. Patel, H. C. Bajaj, R. V. Jasra, (2009) Montmorillonite as a drug delivery system: Intercalation and *in vitro* release of timolol maleate, ***International Journal of Pharmaceutics***, **374**: 53-57.
24. S. Jain, M. Datta, (2014) Montmorillonite-PLGA nanocomposites as an oral extended drug delivery vehicle for venlafaxine hydrochloride, ***Applied Clay Science***, **99**: 42-47.
25. P. García-Guzmán, L. Medina-Torres, F. Calderas, M. J. Bernad-Bernad, J. Gracia-Mora, B. Mena, O. Manero, (2018) Characterization of hybrid microparticles/montmorillonite composite with raspberry-like morphology for atorvastatin controlled release, ***Colloids and Surfaces B: Biointerfaces***, **167**: 397-406.
26. L. S. Eiland, (2012) Glycopyrrolate for chronic drooling in children, ***Clinical Therapeutics***, **34**: 735-742.
27. D. Preiss, P. Berguson, (1983) Dose-response studies on glycopyrrolate and atropine in conscious cardiac patients, ***British Journal of Clinical Pharmacology***, **16**: 523-527.
28. R. Mirakhur, J. Dundee, C. Jones, (1978) Evaluation of the anticholinergic actions of glycopyrronium bromide, ***British Journal of Clinical Pharmacology***, **5**: 77-84.
29. P. R. S. Reddy, K. M. Rao, K. S. V. Rao, Y. Shchipunov, C. S. Ha, (2014) Synthesis of alginate based silver nanocomposite hydrogels for biomedical applications, ***Macromolecular Research***, **22**: 832-842.
30. H. Bera, S. R. Ippagunta, S. Kumar, P. Vangala, (2017) Core-shell alginate-ghatti gum modified montmorillonite composite matrices for stomach-specific flurbiprofen delivery, ***Materials Science and Engineering: C***, **76**: 715-726.
31. R. I. Iliescu, E. Andronescu, C. D. Ghitulica, G. Voicu, A. Ficai, M. Hoteteu, (2014) Montmorillonite-alginate nanocomposite as a drug delivery system-incorporation and *in vitro* release of irinotecan, ***International Journal of Pharmaceutics***, **463**: 184-192.
32. B. D. Kevadiya, G. V. Joshi, H. M. Mody, H. C. Bajaj, (2011) Biopolymer-clay hydrogel composites as drug carrier: Host-guest intercalation and *in vitro* release study of lidocaine hydrochloride, ***Applied Clay Science***, **52**: 364-367.
33. B. D. Kevadiya, G. V. Joshi, H. A. Patel, P. G. Ingole, H. M. Mody, H. C. Bajaj, (2010) Montmorillonite-alginate nanocomposites as a drug delivery system: Intercalation and *in vitro* release of Vitamin B1 and Vitamin B6, ***Journal of Biomaterials Applications***, **25**: 161-177.
34. Q. T. Nguyen, R. Clément, I. Noezar, P. Lochon, (1998) Performances of poly(vinylpyrrolidone-co-vinyl acetate)-cellulose acetate blend membranes in the pervaporation of ethanol-ethyl tert-butyl ether mixtures: Simplified model for flux prediction, ***Separation and Purification Technology***, **13**: 237-245.
35. N. Bailly, M. Thomas, B. Klumperman, (2012) Poly(N-vinylpyrrolidone)-block-poly(vinyl acetate) as a drug delivery vehicle for hydrophobic drugs, ***Biomacromolecules***, **13**: 4109-4117.
36. P. Costa, J. M. S. Lobo, (2001) Modeling and comparison of dissolution profiles, ***European Journal of Pharmaceutical Sciences***, **13**: 123-133.
37. S. O. Dozie-Nwachukwu, Y. Danyuo, J. D. Obayemi, O. S. Odusanya, K. Malatesta, W. O. Soboyejo, (2017) Extraction and encapsulation of prodigiosin in chitosan microspheres for targeted drug delivery, ***Materials Science and Engineering: C***, **71**: 268-278.
38. Y. Seki, K. Yurdakoç, (2006) Adsorption of promethazine hydrochloride with KSF montmorillonite, ***Adsorption***, **12**: 89-100.
39. Q. Wu, Z. Li, H. Hong, K. Yin, L. Tie, (2010) Adsorption and intercalation of ciprofloxacin on montmorillonite, ***Applied Clay Science***, **50**: 204-211.
40. F. Martínez-Gómez, J. Guerrero, B. Matsuhiro, J. Pavez, (2017) *In vitro* release of metformin hydrochloride from sodium alginate/polyvinyl alcohol hydrogels, ***Carbohydrate Polymers***, **155**: 182-191.
41. D. J. D'Sa, D. Lechuga-Ballesteros, H. K. Chan, (2015) Isothermal microcalorimetry of pressurized systems II: Effect of excipient and water ingress on formulation stability of amorphous glycopyrrolate, ***Pharmaceutical Research***, **32**: 714-722.
42. N. N. Sa'adun, R. Subramaniam, R. Kasi, (2014) Development and characterization of poly(1-vinylpyrrolidone-co-vinyl acetate) copolymer based polymer electrolytes, ***The Scientific World Journal***, **7**: 254215.
43. M. A. Güler, M. K. Gök, A. K. Figen, S. Özgümüş, (2015) Swelling, mechanical and mucoadhesion properties of Mt/starch-g-PMAA nanocomposite hydrogels, ***Applied Clay Science***, **112-113**: 44-52.
44. R. Abdeen, N. Salahuddin, (2013) Modified chitosan-clay nanocomposite as a drug delivery system intercalation and *in vitro* release of ibuprofen, ***Journal of Chemistry***, **9**: 576370.
45. H. A. Patel, R. S. Somani, H. C. Bajaj, R. V. Jasra, (2007) Preparation and characterization of phosphonium montmorillonite with enhanced thermal stability, ***Applied Clay Science***, **35**: 194-200.
46. H. Zhang, K. Zou, S. Guo, X. Duan, (2006) Nanostructural drug-inorganic clay composites: Structure, thermal property and *in vitro* release of captopril-intercalated Mg-Al-layered double hydroxides, ***Journal of Solid State Chemistry***, **179**: 1792-1801.
47. M. Z. bin Hussein, Z. Zainal, A. H. Yahaya, D. W. V. Foo, (2002) Controlled release of a plant growth regulator, α-naphthaleneacetate from the lamella of Zn-Al-layered double hydroxide nanocomposite, ***Journal of Controlled Release***, **82**: 417-427.
48. C. D. Nunes, P. D. Vaz, A. C. Fernandes, P. Ferreira, C. C. Romão, M. J. Calhorda, (2007) Loading and delivery of sertraline using inorganic micro and mesoporous materials, ***European Journal of Pharmaceutics and Biopharmaceutics***, **66**: 357-365.
49. F. H. Lin, Y. H. Lee, C. H. Jian, J. M. Wong, M. J. Shieh, C. Y. Wang, (2002) A study of purified montmorillonite intercalated with 5-fluorouracil as drug carrier, ***Biomaterials***, **23**: 1981-1987.

***Bibliographical Sketch**

Dr. (Mrs.) M.C.S. Subha, M.Sc, Ph.D, born in Guntakal, Ananthapur (Dist), A.P, India on 06-06-1957. Graduated in (1977) from Satya Sai Institute of Higher Learning, Ananthapur, A.P, India and obtained M.Sc in Chemistry (1979) from S.V. University, Tirupati, A.P., India. Obtained Ph.D from S.K. University, Ananthapur, A.P, India in 1987 on the topic "Thermodynamic study of binary liquid mixtures" working as UGC-BSR faculty fellow of Chemistry, S. K. University, 28 students are awarded Ph.D and 10 M.Phil, under her guidance and many more are doing research. Published around 187 research papers in national and international journals. She had been to England on commonwealth Academic staff fellowship during 1993-94. She was a recipient of A.P. Govt. Best teacher award. She served S.K. University in many capacities like, Vice-Chancellor (I/c), Rector, Head, Chairman BOS, Warden of ladies hostel, Dean P.G exams, Dean CDC and presently Dean, Faculty of Physical Sciences of S.K. University. Her research interests are Thermodynamics, Polymer membranes, Polymer drug delivery, Chemical Kinetics, etc.